

# Effects of Viscous Dissipation and Micropolar Heat Conduction on MHD Thermally Radiating Flow Along A Vertical Plate

A. Adeniyani<sup>1</sup> and E. O. Fatunmbi<sup>2</sup>

<sup>1</sup>Department of Mathematics, University of Lagos. Akoka, Lagos, Nigeria

<sup>2</sup>Department of Mathematics and Statistics, Federal Polytechnic, Ilaro, Nigeria

## ABSTRACT

The combined influence of micropolar thermal conduction and variable electric conductivity is considered on a boundary layer MHD flow of an electrically conducting polar liquid streaming uniformly over a fixed impermeable vertical plate subjected to variable heat flux in the presence of temperature-dependent thermal conductivity based on Maxwell power law relation. Thermal radiation in cognizance of non-Rosseland approximation is assumed. The nonlinear PDEs governing the flow are converted to ODEs by means of similarity transformation and the obtained equations computed numerically by Runge-Kutta algorithm alongside a shooting technique. The results compared reasonably well with previous studies in the literature. Our findings unveil that the vortex viscosity parameter impedes the fluid motion but accelerates angular velocity, the micropolar conduction parameter cools down the fluid temperature while the velocity ratio impedes angular motion and enhances fluid velocity amongst others.

**KEYWORDS:** Thermal conduction, micropolar fluid, non-Rosseland approximation, viscous dissipation.

## 1.0 INTRODUCTION

In the recent years, the study of non-Newtonian fluids has drawn the attention of scientists and researchers due to its increasing usefulness and practical relevance in many industrial processes. These fluids are particularly important in real industrial applications, such as in polymer engineering, crude oil extraction, food processing etc. It has been observed that the Navier-Stokes equations of classical hydrodynamics cannot adequately explain the complex rheological behaviour that fluids of practical industrial significance exhibit at micro and nano scales. These have led to the development of various micro continuum theories such as simple microfluids, simple deformable directed fluids, polar fluids, anisotropic fluids and micropolar fluids depending on different physical characteristics. However, due to diverse fluid characteristics in nature, all the features of non-Newtonian fluids cannot be contained by a single constitutive model, hence, different models of non-Newtonian fluids have been formulated such as Casson fluid, Jeffery fluid, Maxwell fluid, Johnson-Segalman fluid, Ostwald De-Waele power law fluid and Micropolar fluids etc. (Chen, 2011).

Holt and Fabula (1964), Vogel and Patterson (1964) in their experiments on fluids with small amount of polymeric additives reported that these fluids manifest a reduction in the skin friction near a rigid body. Such phenomenon can neither be captured nor explained by the classical (Newtonian) fluid mechanics. The simple micro-fluids theory developed by Eringen (1964) deals with the class of fluids which possess micro-constituents and are

characterized with certain microscopic influences developing from the local structure and micromotion of the fluid elements. Also, they have the ability to support stress and body moments and are affected by rotation inertia. The crucial points to observe in the formulation of this micro continuum mechanics of Eringen are the introduction of new kinematic quantities; gyration and micro-inertia tensor and are described by twenty-two viscosity and material coefficients (Ariman, Turk and Sylvester, 1973). However, the concept of micro-fluids are too cumbersome when applied to non-trivial, real flow situations. This is because the constitutive equations must be developed in terms of nineteen partial differential equations with nineteen unknowns, hence, the underlying mathematical problem is not easily tractable to solution (Ariman *et al.*, 1973; Eringen, 1966).

In consequence of the mathematical complexities involved in the application of simple micro-fluid concept to the cases of real flow situations, Eringen (1966, 1972) formulated a subclass of microfluids known as micropolar fluid and as well derived the constitutive equations for the theory of thermo-micropolar fluids. Micropolar fluids are important branch of non-Newtonian fluids dynamics with microstructure and constitute a substantial generalization of the Navier-Stokes model. By this theory, each element of the fluid is associated to two sets of degrees of freedom, viz: translatory degrees of freedom, giving rise to mass transport, and rotation/stretch, permitting the particles to undergo independent intrinsic spins and homogenous deformation (Ariman *et al.*, 1973). These fluids provide a mathematical framework for investigating many complicated and complex fluids such as suspension solution, liquid crystal, animal blood, colloidal fluids etc. (Ahmadi, 1976; Hayat *et al.*, 2011). Its applications in a number of industrial processes, such as extrusion of polymer fluids, the flow of exotic lubricants, colloidal suspensions and the cooling of metallic plate in water bath have also boosted the interest of researchers in studying them (Rahman 2009)). A detailed review, on the theory and applications of micropolar fluids, was given by Lukaszewicz (1999). The boundary layer flow of such fluids was first studied by Peddieson and McNitt (1970) and Wilson (1970).

The fluid flow induced by stretching sheet be it vertical or horizontal has significant usefulness in engineering and industrial operations, for instance, drawing of plastic sheet, glass blowing, hot rolling, the cooling of metallic plate in a bath, annealing and thinning of copper wires, textile and paper productions etc. Particularly, in many metallurgical operations including the cooling of continuous strips or filaments drawn through a quiescent fluid, the strips are often stretched. In such situations, the quality of the final product is determined to a great extent on the rate of stretching and that of cooling. When such strips are drawn in an electrically conducting fluid subjected to a magnetic field, the rate of cooling can be controlled and consequently a final product of desired characteristics can be obtained. Pioneering the work on boundary layer flow caused by stretching sheet, Crane (1970) offered a similarity solution in closed analytical form to a linearly stretching sheet on the steady two-dimensional sheet while Gupta and Gupta (1977) extended the work of Crane to include heat and mass transfer on stretching sheet with suction or blowing. Eldabe *et al.* (2003) discussed MHD flow of a micropolar fluid past a stretching sheet with heat transfer.

Reddy (2012) reported on heat generation and thermal radiation effects over a stretching sheet in a micropolar fluid

Fatunmbi and Fenuga (2017) studied MHD micropolar fluid flow over a permeable stretching sheet in the presence of variable viscosity and thermal conductivity with Soret and Dufour effects in a Darcy-Forchheimer porous medium

## 2.0 PROBLEM FORMULATION

Consider a steady, two-dimensional, viscous, incompressible, electrically conducting micropolar fluid flow over an impermeable vertical stretching plate with micropolar heat conduction and viscous dissipation. The cartesian coordinate system and the geometry of the flow is as illustrated in Figure 1. The flow is assumed to be in the  $x$  direction which is taken along the vertical sheet with  $y$  axis is normal to it. A uniform magnetic field  $\mathbf{B}=(0, B_0, 0)$  of strength  $B_0$  is applied normal to the flow direction. Thermal radiation in cognizance of non-Rosseland approximation is assumed. It is assumed also that the magnetic Reynolds number is sufficiently small such that the induced magnetic field is negligible as compared to the applied magnetic field. In view of the aforementioned assumptions the boundary layer approximations, the governing boundary layer continuity, momentum, microrotation and energy are respectively given as:

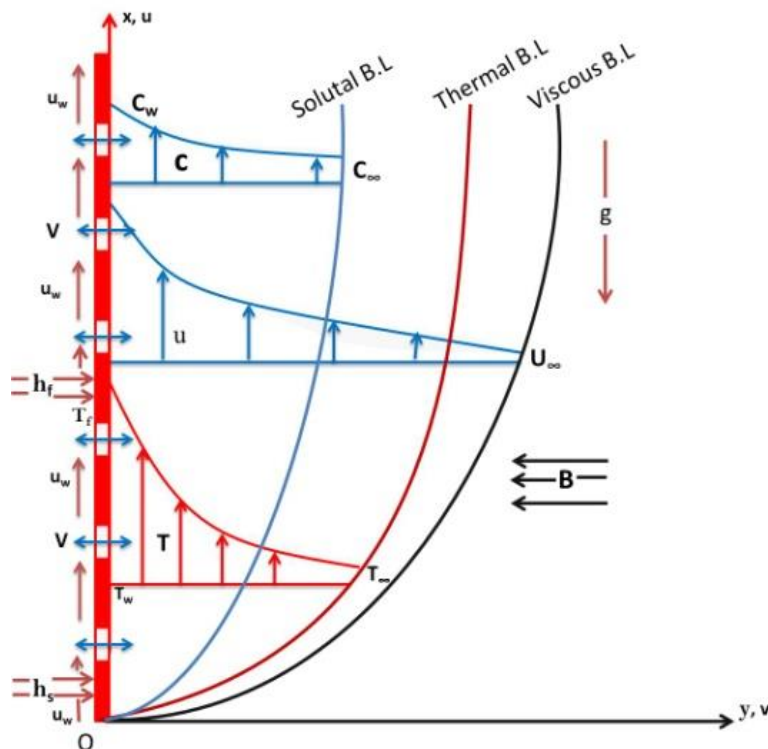


**Figure 1:** Flow Geometry and Coordinate System

## Governing equations

$$\frac{\partial u}{\partial x} + \frac{\partial v}{\partial y} = 0$$

(1)

$$u \frac{\partial u}{\partial x} + v \frac{\partial u}{\partial y} = \frac{\mu + \kappa}{\rho} \frac{\partial^2 u}{\partial y^2} + \frac{\kappa}{\rho} \frac{\partial N}{\partial y} + g\beta(T - T_\infty) - \frac{\sigma_\epsilon B^2(x)}{\rho} (u - U_\infty) \quad (2)$$

$$\rho j \left( u \frac{\partial N}{\partial x} + v \frac{\partial N}{\partial y} \right) = \gamma \frac{\partial^2 N}{\partial y^2} - \kappa \left( 2N + \frac{\partial u}{\partial y} \right) \quad (3)$$

$$\rho C_p \left( u \frac{\partial T}{\partial x} + v \frac{\partial T}{\partial y} \right) = \frac{\partial}{\partial y} \left( k(T) \frac{\partial T}{\partial y} \right) + (\mu + \kappa) \left( \frac{\partial u}{\partial y} \right)^2 - 4\epsilon \sigma^* T^4 + q^{iv} \quad (4)$$

$$q^{iv} = \lambda^* \left( \frac{\partial T}{\partial x} \frac{\partial N}{\partial y} - \frac{\partial T}{\partial y} \frac{\partial N}{\partial x} \right)$$

(5)

$\lambda^*$  is micropolar heat conduction coefficient.

## Boundary conditions

$$\left. \begin{aligned} u = 0, v = 0, N = -m \frac{\partial u}{\partial y}, -k \frac{\partial T}{\partial y} = q_w \quad @ \quad y = 0 \\ u \rightarrow U_\infty, \quad N \rightarrow 0, \quad T \rightarrow T_\infty \quad as \quad y \rightarrow \infty \end{aligned} \right\} \quad (6)$$

## Local shear wall parameter, wall couple stress, wall heat transfer rate

$$\tau_w = \left[ (\mu + \kappa) \frac{\partial u}{\partial y} + \kappa N \right]_{y=0}, \quad M_w = \gamma \frac{\partial N}{\partial y} \Big|_{y=0}, \quad q_w = -k \frac{\partial T}{\partial y} \Big|_{y=0} - q_r \Big|_{y=0} \quad (7)$$

Local skin-friction coefficient, local couple stress coefficient, local Nusselt number:

$$Cf = \frac{2\tau_w}{\rho U_0^2}, \quad Cs = \frac{2xM_w}{\rho j U_0^2}, \quad Nu_x = \frac{xq_w}{k\Delta T}$$

(8)

## Non-dimensionless equations

$$\eta = y \sqrt{\frac{U_0}{2\nu x}}, \quad \psi = \sqrt{2\nu U_0 x} f(\eta), \quad N = \sqrt{\frac{U_0^3}{2\nu x}} h, \quad \theta(\eta) = \frac{T - T_\infty}{T_w - T_\infty}, \quad (9)$$

where  $\psi(x, y), U_0, \Delta T = \frac{q_w(x)}{k} \sqrt{\frac{2\nu x}{U_0}}$  are respectively the stream function, some reference velocity and the characteristic temperature difference. The prescribed heat flux is taken as  $q_w = q_{wo}x^\lambda$ , while  $q_{wo}$  is the characteristic heat transfer flux constant.

$$(1+K)f''' + ff'' + Kh' + Gr\theta(\eta) - M(f'^2 - \varepsilon) = 0 \quad (10)$$

$$\left(1 + \frac{K}{2}\right)h'' + h'f - H(2h + f'') = 0 \quad (11)$$

$$\frac{1}{Pr} \left\{ \theta'' + n\theta_r(1 + \theta_r\theta)^{-1} \theta'^2 \right\} + \theta'f - (2\lambda + 1)\theta f' + (1+K)Ec f''^2 + R(1 + \theta_r\theta)^4 + \alpha^* [(2\lambda + 1)\theta h' - h\theta'] = 0 \quad (12)$$

$$\left. \begin{aligned} \eta = 0: & \quad f(0) = 0, f'(0) = 0, h(0) = -m, \theta'(0) = -1 \\ \eta \rightarrow 0: & \quad f'(\infty) = \varepsilon, h(\infty) = 0, \theta(\infty) = 0 \end{aligned} \right\} \quad (13)$$

### 3.0 Results and Discussion

The Boundary Value Problem (BVP) equations (10-13) are integrated via shooting technique cum Runge-Kutta method.

For proper understanding of the behaviour of the fluid flow, a computational analysis has been carried out for the dimensionless velocity, temperature and microrotation profiles across the boundary layer and presented through graphs and table.

Table 1 illustrates the effects of the material (micropolar) parameter  $K$ ,  $\alpha$ , velocity ratio parameter  $\beta$ , micropolar heat conduction parameter  $\lambda$ , magnetic field parameter  $M$  and Eckert number  $Ec$  and on the skin friction coefficient  $f''(0)$ , the local Nusselt number (rate of heat transfer)  $-\theta(0)$  and the wall couple stress  $g'(0)$ . From this table, it is observed that the skin friction coefficient reduces with an increase in both  $K$  and  $\alpha$  whereas the parameters  $\beta, \lambda, M$  and  $Ec$  enhance the skin friction coefficient  $f''(0)$ . Similarly, the rate of heat transfer increases with a rise in  $\beta, \lambda, M$  and  $Ec$  while the trend is reversed with an increase in  $K$  and  $\alpha$ . In addition, the effect of  $K, \alpha$  and  $\lambda$  is to reduce the couples stress  $g'(0)$  whereas  $\beta, M$  and  $Ec$  enhance the couple stress  $g'(0)$ .

Figures 2-4 illustrates the effects of the material parameter  $K$  on the the velocity, microrotation and temperature profiles across the boundary layer. Figure 2 shows that there is a decrease in the fluid velocity as well as in the hydrodynamic boundary layer thickness as  $K$  increases. Similarly, the microrotation distribution across the boundary layer reduces as  $K$  rises with the negative values of the microrotation implying reverse spinning of the micro-particles as shown in Figures 3. On the other hand,

the temperature increases and the thermal boundary layer thickens with a rise in the material parameter  $K$  as depicted in Figure 4.

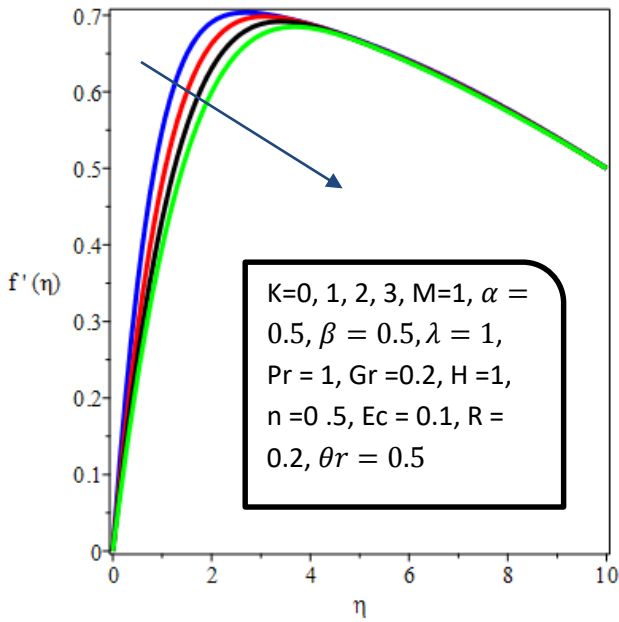
**Table 1:** Values of skin friction coefficients, Nusselt number and wall couple stress for  $K, \alpha, \beta, \lambda, M$  and  $Ec$

$K$	$\alpha$	$\beta$	$\lambda$	$M$	$Ec$	$f''(0)$	$-\theta'(0)$	$g'(0)$	
0.7	1.0	0.5	1.0	0.2	0.5	0.724088	0.029322	0.161150	
1.0						0.681170	0.027836	0.142959	
1.2						0.656447	0.024704	0.133001	
1.0	0.2					0.674963	0.214807	0.141140	
	1.0					0.681170	0.027836	0.142959	
	2.5					0.686525	-	0.144546	
	1.0	0.5				0.681170	0.027836	0.142959	
		0.6				0.759453	0.091758	0.159103	
		0.7				0.835644	0.143476	0.174812	
		0.5	1.0			0.681170	0.027836	0.142959	
			1.5			0.671784	0.157725	0.140801	
			2.5			0.661045	0.307699	0.138234	
				0.2		0.487975	-	0.082186	
						0.5	0.553762	0.055152	0.100828
						1.0	0.681170	-	0.142959
							0.010992		
							0.027836		
			1.0	0.2	0.05	0.679422	0.066440	0.142451	
					0.5	0.683113	-	0.143515	
					1.5	0.686971	0.012312	0.144588	
							-		
							0.085196		

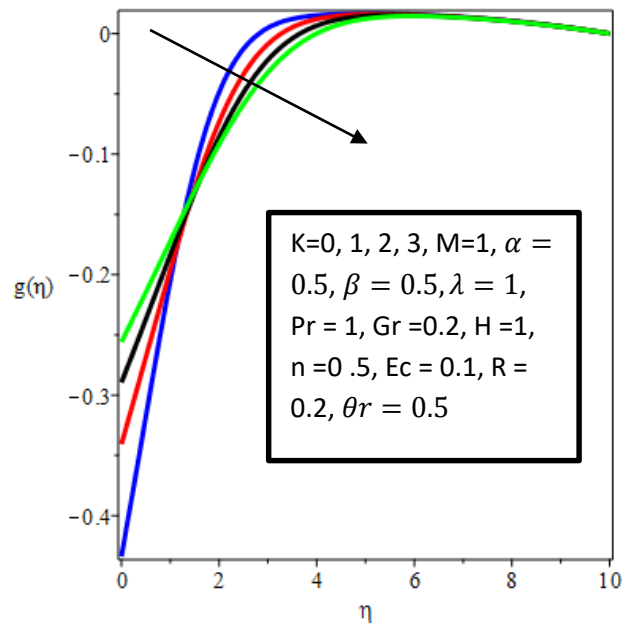
Figure 5 shows the effect of  $\alpha$  on the temperature profiles. It is shown that an increase in  $\alpha$  causes the temperature profiles as well the thermal boundary layer to increase. Moreover, it is observed that the rate of transport reduces with the increasing distance  $\eta$  from the sheet as depicted in Figure 5. The influence of the micropolar heat conduction parameter  $\lambda$  on the temperature profiles shows that the temperature falls as  $\lambda$  increases. In addition, the thermal boundary layer thins out as  $\lambda$  rises as shown in Figure 6.

Figure 7 describes the effect of the velocity ratio parameter  $\beta$  on the velocity. Evidently, there is a rise in the velocity profiles as  $\beta$  increases due to the thickening of the hydrodynamic boundary layer. However, the temperature and microrotation profiles as well as the thermal and the microrotation boundary layer thicknesses decrease with an increase in  $\beta$  as displayed in Figures 8 and 9. Also, the microrotation effect displays a reverse spinning of the micro-particles as shown in Figure 9.

Figures 10-12 illustrate the effect of the radiation parameter  $R$ , Eckert number  $Ec$  and the variable thermal conductivity parameter  $\theta_r$  on the temperature profiles across the boundary layer. Clearly, an increase in  $R, Ec$  and  $\theta_r$  cause a rise in the temperature profiles and the thickening of the thermal boundary layer thickness as depicted in these Figures. Figure 13 shows the effect of Prandtl number  $Pr$  on the temperature distribution across the boundary layer. Evidently, an increase in the magnitude of the Prandtl number causes a dampen effect on the temperature profiles and reduces the thermal boundary layer thickness. Thus, increasing  $Pr$  implies reducing the thermal boundary layer thickness which in turn lowers the average temperature within the boundary layer. Increasing Prandtl parameter can therefore be applied to enhance the rate of cooling as fluids with moderate Prandtl number creates higher conductivities and such heat diffuses quickly away from the heated plate than for higher values of  $Pr$ .



**Fig. 2.** Effect of  $K$  on velocity



**Fig. 3.** Effect of  $K$  on

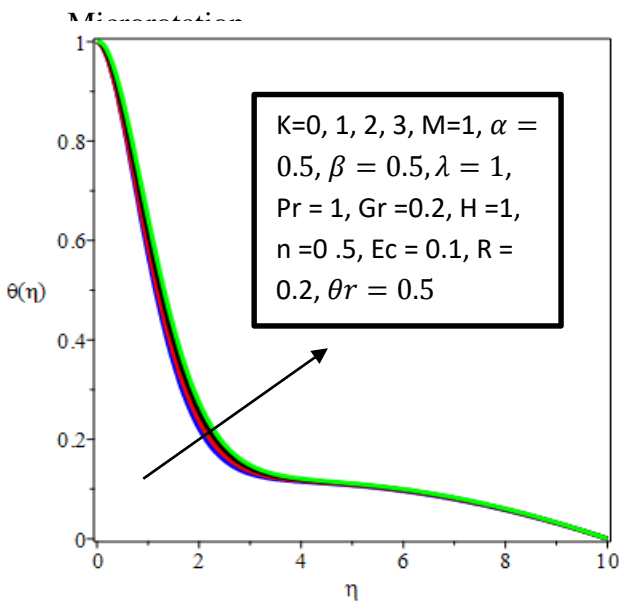


**Fig. 4.** Effect of  $K$  on Temperature

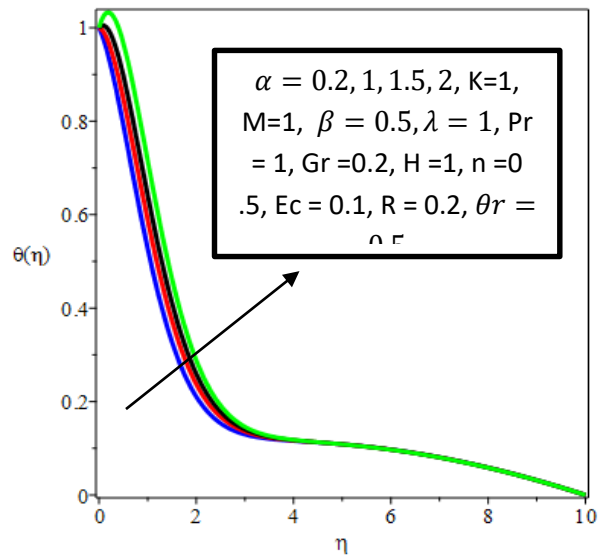


**Fig. 5.** Effect  $\alpha$  on Temperature

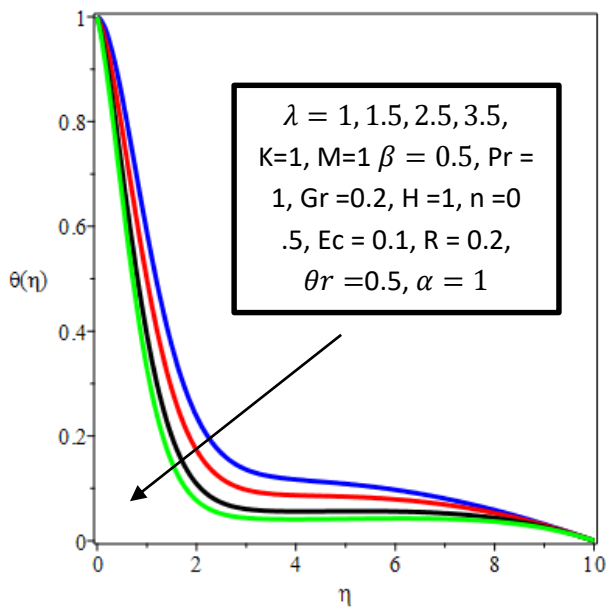


**Fig. 6.** Effect of  $\lambda$  on Temperature

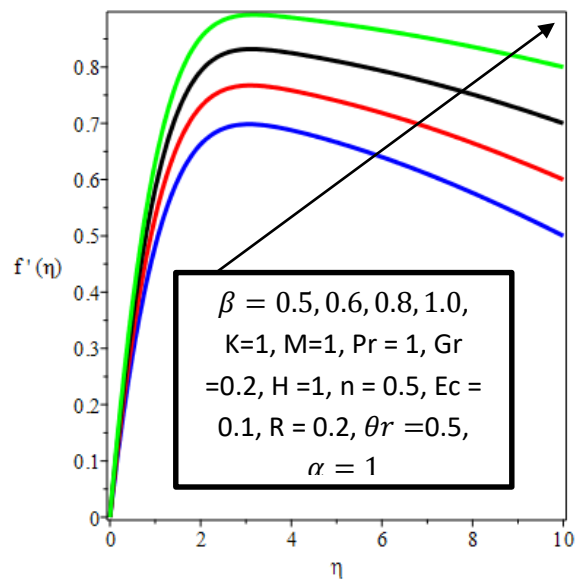


**Fig.7.** Effect of  $\beta$  on velocity

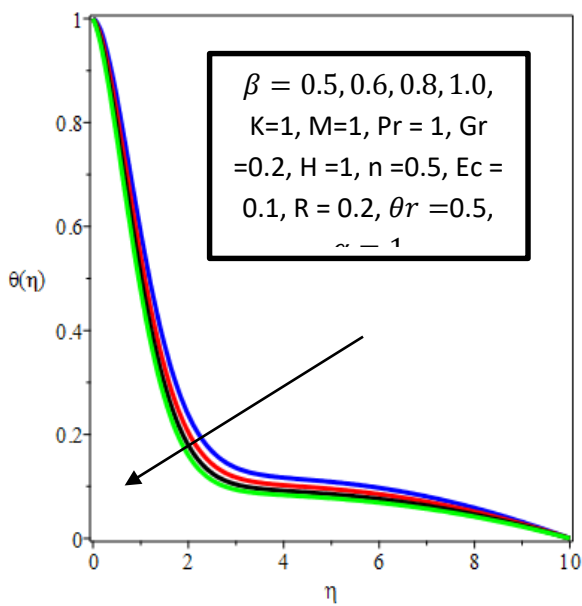


**Fig. 8.** Effect of  $\beta$  on Temperature

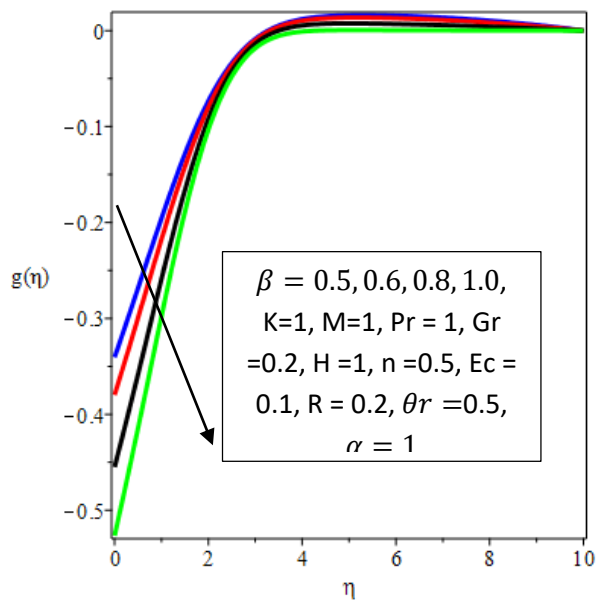


**Fig. 9.** Effect of  $\beta$  on Microrotation

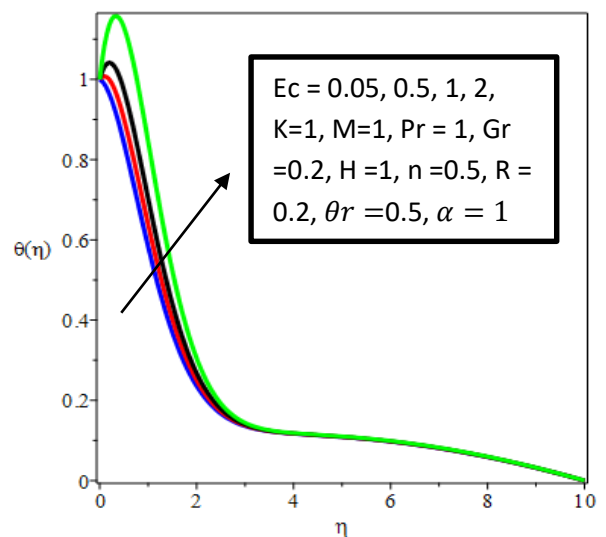
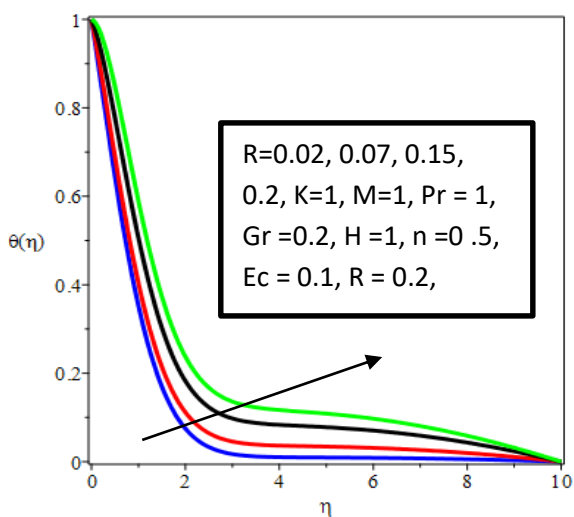




**Fig. 10.** Effect of  $R$  on Temperature

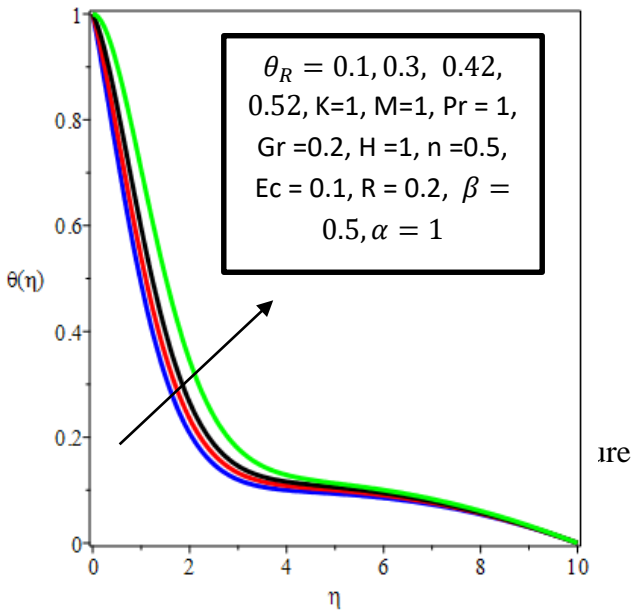


**Fig. 12.** Effect of  $\theta_R$  on Temperature

**Fig. 11.** Effect of  $Ec$  on Temperature

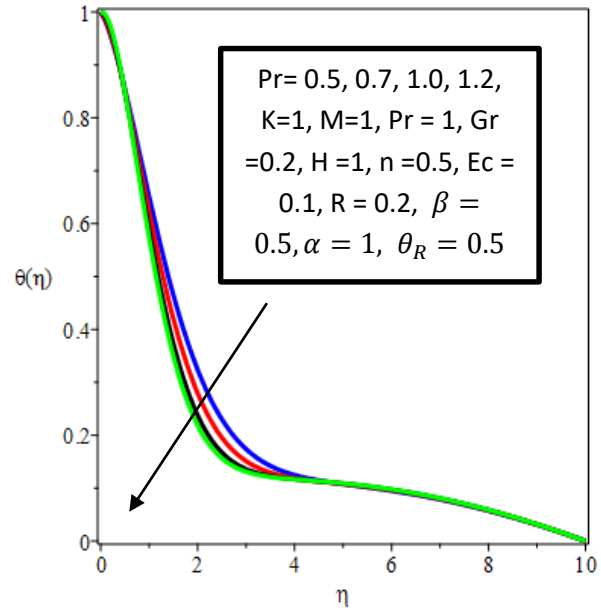


**Fig. 13.** Effect of  $Pr$  on Temperature

## REFERENCES

- Ahmadi, G. (1976). Self-similar solution of incompressible micropolar boundary layer flow over a semi-infinite plate, *Int. J. Engng Sci*, 14, 639-646.
- Chen, J., Liang, C. and Lee J. D. (2011). Theory and simulation of micropolar fluid dynamics, *J. Nanoengineering and Nanosystems*, 224, 31-39 (2011).
- Crane, L. J. (1970) Flow past a stretching plate, *Communicatioes Breves*, 21, 645-647.
- Eldabe, N. T., Elshehawey, E. F., Elbarbary, M. E., Elgazery, N. S.:(2003). Chebyshev finite difference method for MHD flow of a micropolar fluid past a stretching sheet with heat transfer, *Journal of Applied Mathematics and Computation*, 160, 437-450.
- Eringen, A. C. (1966). Theory of micropolar fluids, *J. Math. Anal. Appl.*, 16: 1-18.
- Eringen, A. C. (1972) Theory of thermo-microfluids, *Journal of Mathematical Analysis and Applications*, 38, 480-496 (1972).
- Fatunmbi, E. O and Fenuga, O. J. (2017). MHD micropolar fluid flow over a permeable stretching sheet in the presence of variable viscosity and thermal conductivity with Soret and Dufour effects, *International Journal of Mathematical Analysis and Optimization: Theory and Applications*, 2017, 211- 232.

- Gupta, P. S., Gupta, A. S. (1977). Heat and mass transfer on a stretching sheet with suction or blowing, *Can. J. Chem. Eng*, 55: 744-746.
- Hayat, T., Shehzad, S. A. and Qasim, M. (2011). Mixed convection flow of a micropolar fluid with radiation and chemical reaction, *Int J. Numer Meth*, 67, 1418-1436
- Hoyt, J. W. and Fabula, A. G., (1964). The Effects of Additives on Fluid Friction, US Naval Ordnance Test Station Report.
- Lukaszewicz, G. (2009). *Micropolar fluids: Theory and Applications*, 1st Ed., Birkhauser, Boston,
- Peddieson, J., McNitt, R. P. (1970). Boundary layer theory for micropolar fluid, *Recent Adv. Engng Sci.*, 5, 405.
- Reddy, M. G. (2012). Heat generation and thermal radiation effects over a stretching sheet in a micropolar fluid, *International Scholarly Research Networks*, 2012, 1-6 doi.org./10.5402/2012/795814.
- Rahman, M. M., 2009. Convective flows of micropolar fluids from radiate isothermal porous surface with viscous dissipation and joule heating, *Commun Nonlinear Sci. Numer Simulat*, 14, 3018-3030.